J Mater Sci: Mater Med (2009) 20:265–269
DOI 10.1007/s10856-008-3568-1

Fabrication of bioglass infiltrated Al_2O_3–(m-ZrO_2) composites

Ho-Yeon Song · Swapan Kumar Sarkar · Min Sung Kim · Young Ki Min · Yang Hun Mo · Byong-Taek Lee

Received: 18 February 2008 / Accepted: 18 August 2008 / Published online: 3 September 2008

Abstract Using 80 vol.% of poly methyl methacrylate (PMMA) as a pore-forming agent to obtain interconnected porous bodies, porous Al_2O_3–(m-ZrO_2) bodies were successfully fabricated. The pores were about 200 μm in diameter and were homogeneously dispersed in the Al_2O_3–25 vol.% (m-ZrO_2) matrix. To obtain Al_2O_3–(m-ZrO_2)/bioglass composites, the molten bioglass was infiltrated into porous Al_2O_3–(m-ZrO_2) bodies at 1400°C. The material properties of the Al_2O_3–(m-ZrO_2)/bioglass composites, such as relative density, hardness, compressive strength, fracture toughness and elastic modulus were investigated.

1 Introduction

In search of suitable replacement or supporting material for human hard tissue, researchers have been investigating for decades on different materials. Extremely inert material in the physiological condition like the Al_2O_3 and ZrO_2 ceramics has gained attention for a range of applications [1, 2]. But lack of bioactivity and inability to conform to the material properties of living hard tissue, specially the elastic modulus (too high) and fracture toughness (low enough) has lead researchers to design new materials that can exhibit superior biological response and at the same time have good mechanical properties [3]. Calcium phosphate based materials, that resemble the material of the bone itself was a promising candidate [4]. Recently bioactive glass materials, with a better biological response than the calcium phosphate based materials, have been investigated for this purpose [5, 6]. Bioactive glasses have been investigated and found to be a promising alternative as materials to repair or replace damaged parts of human bones and teeth due to their good biocompatibility and excellent bioactivity [7–9]. Several kinds of bioglasses were reported among which bioglass 58S has shown good bonding to human bone as well as to soft tissue and resorbed inside body relatively fast, providing a very good extent of bioactivity [10, 11]. However, the biocompatibility and bone bonding are not all of the requirements for bone repair and replacement materials. Bioglass showed low mechanical properties, especially the fracture toughness [12, 13]. Thus, there is a strong impetus to improve the mechanical properties of bioactive ceramics so that they can be used in load-bearing hard tissue.

There are some reports attempting to improve the mechanical properties of bioglass using HAp nanofibres [14], metal fibre [15] and a Fe–Cr alloy [16]. However, they showed limitations in the improvement of the mechanical properties or degrade the excellent biocompatibility of the bioglass. As already said the Al_2O_3 and ZrO_2 ceramics have received a lot of attentions to use for implants such as prostheses, dental materials and femoral head due to their good biocompatibility and corrosion resistance, excellent chemical stability, and outstanding mechanical properties [17–19]. Thus, they can be considered as suitable reinforcement materials for bioglass, especially in the purpose where high corrosion resistance is required. The combination of Al_2O_3 and m-ZrO_2 is considered for composites due to the fact that this composite can introduce some interesting features like microcracks at grain boundary, residual stress development, etc., which can modify the behaviour of the material positively in terms of mechanical performance [17].

H.-Y. Song · S. K. Sarkar · M. S. Kim · Y. K. Min · Y. H. Mo · B.-T. Lee (✉)
School of Medicine, Soonchunhyang University, 366-1, Ssangyoung-dong, Cheonan, Chungnam 330-090, South Korea
e-mail: lbt@sch.ac.kr

The present work described a new method to fabricate Al_2O_3–(m-ZrO_2)/bioglass composites using melt infiltration of bioglass into porous Al_2O_3–(m-ZrO_2) bodies. Porous composites were fabricated first using replica method by driving away PMMA micro-sphere within the Al_2O_3–(m-ZrO_2) matrix and creating interconnected spherical pores. Detailed microstructure and mechanical properties of Al_2O_3–(m-ZrO_2)/bioglass composites were investigated.

2 Experimental procedure

2.1 Material processing

As starting materials, Al_2O_3 (300 nm, Sumitomo, Japan), monoclinic Zirconia (m-ZrO_2) (80 nm, Tosho, Japan), bioglass 58S (Shofu Inc., Kyoto, Japan) and poly methyl methacrylate (PMMA) (200 μm, LG chemical company, Korea) as pore-forming agent powders were used. The processing of the composites were done in two steps; initially making the Al_2O_3–(m-ZrO_2) porous body with interconnected pore and then by subsequent bioglass infiltration into the porous body. To make porous Al_2O_3–(m-ZrO_2) bodies, first, 75 vol.% Al_2O_3 and 25 vol.% ZrO_2 powders were mixed for 24 h by wet ball-milling using Al_2O_3 balls. After drying, the mixed ceramic powders and PMMA powder were mixed for 24 h by dry ball-milling using the same Al_2O_3 balls. The composition of ceramic powders and PMMA was 20/80 vol.% to ensure sufficient porosity as well as interconnectivity of the pores. The mixed powders were then compacted to form pellets (diameter 1.3 cm) by uni-axial press. The green pellets were burnt out in an air atmosphere at 1000°C to drive out the PMMA and form the intended pores. Finally, the burnout samples were sintered at 1500°C in an air atmosphere to obtain porous Al_2O_3–(m-ZrO_2) bodies.

To infiltrate bioglass into the porous composites, it was kept in a mould with one end open. Subsequently, sufficient amount of bioglass powder was put on the top of the porous Al_2O_3–(m-ZrO_2) bodies and were put into the furnace and was heated to 1400°C. To ensure that the molten bioglass was completely infiltrated into the porous Al_2O_3–(m-ZrO_2) bodies the dwelling time at this temperature was set to 60 min. The bioglass on the outside of the samples was removed by polishing to take Al_2O_3–(m-ZrO_2)/bioglass composites.

2.2 Mechanical properties evaluation

The relative density of Al_2O_3–(m-ZrO_2)/bioglass composites was measured by the Archimedes method. The pore size and microstructure of the porous Al_2O_3–(m-ZrO_2) bodies and Al_2O_3–(m-ZrO_2)/bioglass composites were investigated by scanning electron microscopy (SEM, JSM-635F, JEOL). To identify the crystal structure and phases, an X-ray diffractometer (XRD, D/MAX-250, Rigaku, Japan) was used. The hardness and fracture toughness were measured using a Vickers hardness tester (Hv-112, Akashi, Japan) by indentation with a load of 0.5 kg. The specimens with a dimension of $\Phi 12 \times 4$ mm^3 were used for a compression test using a universal testing machine (UnitechTM, R&B, Korea) with a crosshead speed of 0.5 mm/min in ambient conditions. The stress–strain curve obtained was used to determine the mechanical properties. The compressive strength and elastic modulus were determined from the maximum load recorded and from the slope at the initial stage, respectively. Five specimens were tested for each condition.

3 Results and discussion

Figure 1 showed TG & DTA profiles of 58S bioglass. In the TG profile, the weight percentage of 58S bioglass decreased as the temperature increased to 430°C. The amount of 58S bioglass decreased about 0.26 wt.%, which was mainly due to the desorption of physically and chemically adhered moisture or gaseous materials. From the DTA profile, it was evident that an endothermic reaction had occurred at around 771.8–842.5°C. An associated weight loss, though negligible, was also observed in the same temperature range. This indicates a change in the chemical composition in the glassial phase of the 58S bioglass. The nominal composition of the 58S bioglass powder in mol% was 60% SiO_2, 36% CaO and 4% P_2O_5, as shown in Table 1.

Figure 2 showed SEM micrographs of (a) porous Al_2O_3–(m-ZrO_2) composites and (b) Al_2O_3–(m-ZrO_2)/

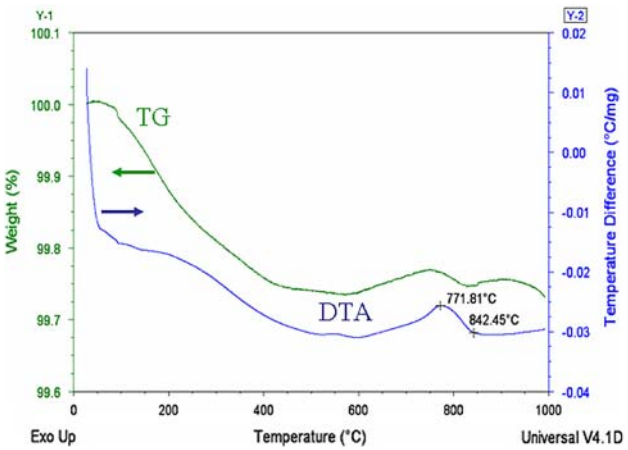

Fig. 1 TG & DTA profiles of 58S bioglass

Table 1 The nominal composition of the 58S bioglass powder in mol%

SiO_2	CaO	P_2O_5
60%	36%	4%

bioglass composites. Figure 2a revealed that the PMMA, which was used as a pore-forming agent, was completely removed after the burning-out and sintering processes. The impression of the PMMA with in the Al_2O_3–(m-ZrO_2) matrix was intact and form spherical shaped pores. The pores were around 200 μm in diameter and were homogeneously dispersed in the Al_2O_3–(m-ZrO_2) matrix. The close proximity of the PMMA spheres with each other was the single most important factor for the interconnectivity of the pores, which was ensured by adding as high as 80 vol. % of PMMA in the green compact. But the same fact also contributed to the very thin frame region of the Al_2O_3–(m-ZrO_2) matrix and thereby degrading the material properties. From the Fig. 2a both the interconnected porosity and the thin frame were evident. Interconnectivity of the pores is an important parameter for the sound infiltration process. It is also important because the interconnectivity of the pores will finally dictate the proliferation and in-growth of the bone cells inside the composites. Figure 2b showed SEM image of polished surface of the composites after the infiltration of bioglass. The bioglass was completely infiltrated into the porous Al_2O_3–(m-ZrO_2) composites which were interconnected to each other. However, a few residual pores were observed completely devoid of bioglass, which was due to the lack of interconnectivity and being stand alone pores.

Figure 3 showed XRD profiles of (a) raw bioglass, (b) porous Al_2O_3–(m-ZrO_2) composites and (c) Al_2O_3–(m-ZrO_2)/bioglass composites. After infiltration of bioglass into porous Al_2O_3–(m-ZrO_2) composites, a $Ca_7Si_2P_2O_{16}$ peak as a new phase, with sharp, strong intensity was detected. The Ca_2SiO_4 and Ca_3SiO_5 phases, which appeared

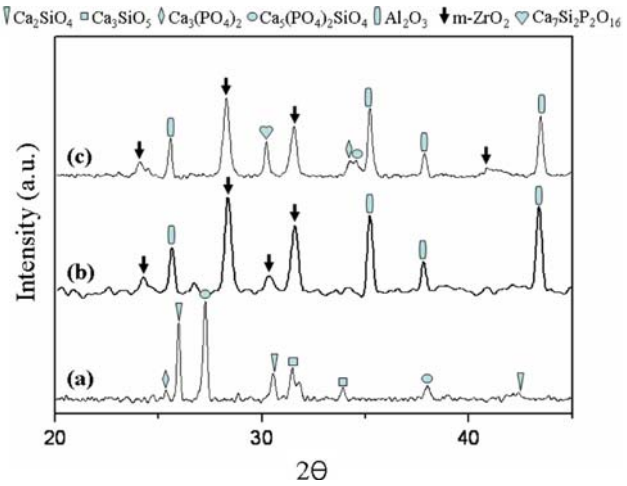

Fig. 3 XRD profiles of (**a**) raw bioglass, (**b**) porous Al_2O_3–(m-ZrO_2) composites and (**c**) Al_2O_3–(m-ZrO_2)/bioglass composites

in the raw bioglass (a), were not observed. The formation of the $Ca_7Si_2P_2O_{16}$ phase could be explained due to the reaction of Ca_2SiO_4 and Ca_3SiO_5 with $Ca_3(PO_4)_2$ phases with the following equation:

$$Ca_2SiO_4 + Ca_3SiO_5 + Ca_3(PO_4)_2 = Ca_7Si_2P_2O_{16} + CaO$$

Figure 4 shows SEM fracture surfaces of Al_2O_3–(m-ZrO_2)/bioglass composites. In Fig. 4a, the fracture surface showed a clear bimodal fracture behaviour with a rough surface with the Al_2O_3–(m-ZrO_2) frame indicating an intergranular fracture mode and with a flat and smooth fracture surface in the bioglass phase indicating a transgranular fracture mode. The intergranula fracture mode of the frame region increased the fracture toughness of the composites. From Fig. 4b, the enlarged image showed that there were a very low presence of interfacial cracks and debonding of the Al_2O_3–(m-ZrO_2) matrix material and the infiltrated bioglass phase. This indicated

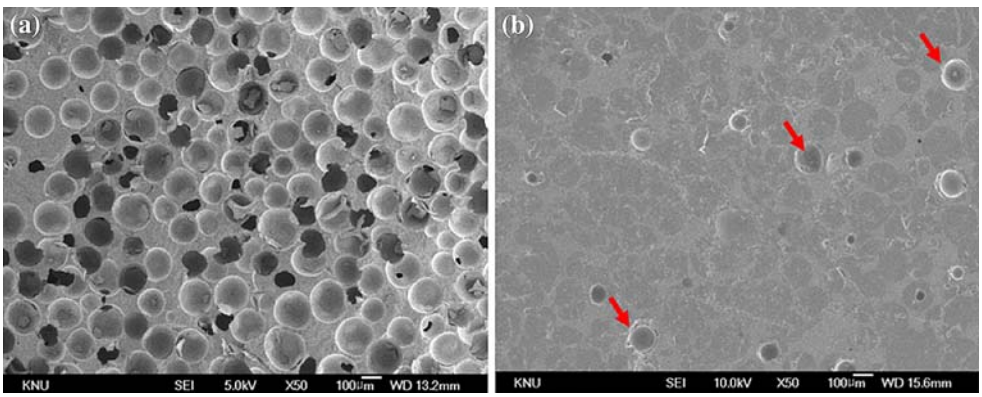

Fig. 2 SEM micrographs of (**a**) porous Al_2O_3–(m-ZrO_2) composites and (**b**) Al_2O_3–(m-ZrO_2)/bioglass composites

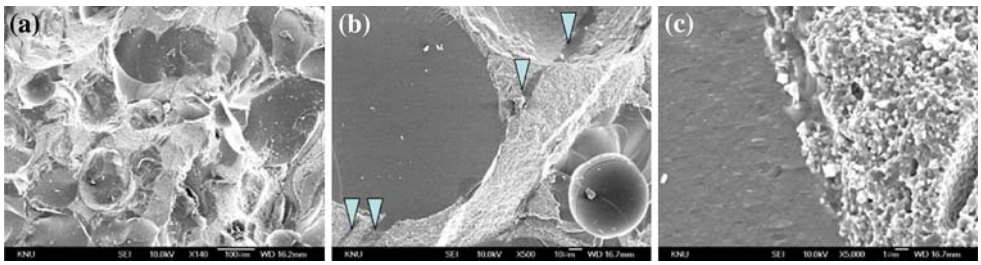

Fig. 4 SEM fracture surfaces of Al_2O_3–(m-ZrO_2)/bioglass composites (**a**) low magnification, (**b**) enlarged image and (**c**) enlarged image of interface between Al_2O_3–(m-ZrO_2) and bioglass

that the bioglass was well infiltrated inside the porous body and the bonding between the ceramics and bioglass was strong. This can be observed more clearly in Fig. 4c. This observation indicated that their interfaces existed with strong bonding. However, some micro-cracks were found at the Al_2O_3–(m-ZrO_2) pore frame as indicated by arrowheads in Fig. 4b. This was because, with a very high content (80%) of porosity, the Al_2O_3–(m-ZrO_2) porous composites before infiltration was mechanically not so strong as expected as it underwent a significant extent of shrinkage. However, this contributed a limited drawback to the composite's desired mechanical performance.

Figure 5 shows the enlarged SEM fracture surfaces of Al_2O_3–(m-ZrO_2)/bioglass composites. In Fig. 5a, high magnification of the Al_2O_3–(m-ZrO_2) matrix, the microstructure was observed homogeneous with the same grain size of <0.7 μm in diameter. The main fracture mode was an intergranular type, although a few flat regions appeared due to the transgranular fracture. From previous work, improved fracture and crack propagation behavior in this system was reported [20]. Due to the dispersion of m-ZrO_2 grains in the Al_2O_3 matrix, the interfaces between Al_2O_3 and m-ZrO_2 grains may be more interacting with crack propagation or fracture surface generation because of the existence of micro-cracks during the formation of twins. Figure 5b, the high magnification image of the bioglass area, showed the typical flat surface of the bioglass.

The material properties of Al_2O_3–(m-ZrO_2)/bioglass composites were shown in Table 2. The fracture toughness of the composites was measured by the indentation method using Evan's equation, which is:

$$K_{IC} = 0.16Ha^{1/2}(c/a)^{-3/2}$$

where H is the Vickers hardness, a is half of the indentation diagonal, and c is half of the crack length from the indentation center. The values of relative density, hardness, compressive strength, fracture toughness and elastic modulus of the composites, were 96.6%, 767 Hv, 375 MPa, 2.35 MPa $m^{1/2}$ and 86.8 GPa, respectively. In general, the maximum fracture toughness of the bioglass reported in the literature varied from 0.96 to 1 MPa $m^{1/2}$ [12, 21]. Thus, the high values of fracture toughness and elastic modulus attained in the present work were encouraging compared to those of dense bioglass [21].

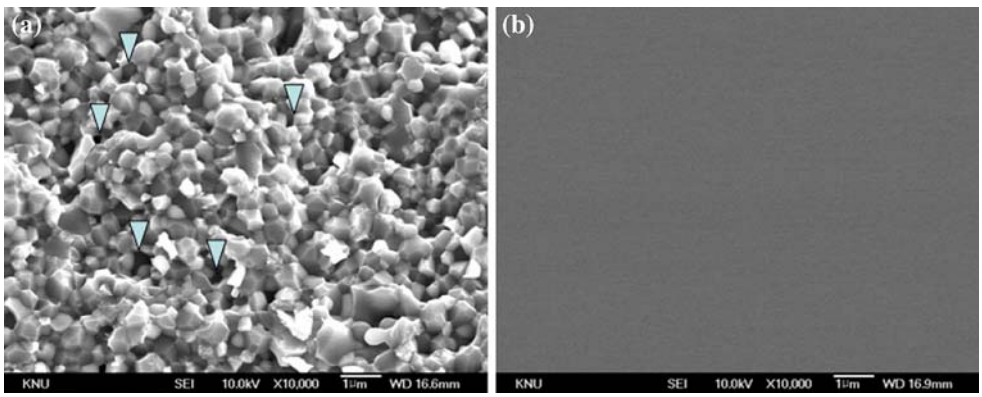

Fig. 5 SEM fracture surfaces of Al_2O_3–(m-ZrO_2)/bioglass composites (**a**) high magnification of pore frame and (**b**) high magnification of bioglass area

Table 2 The material properties of Al_2O_3–(m-ZrO_2)/bioglass composites and dense bioglass

	Relative density (%)	Hardness (Hv)	Compressive strength (MPa)	Fracture toughness (MPa $m^{1/2}$)	Elastic modulus (GPa)
Composites	96.6	767 ± 1	375 ± 1	2.35 ± 0.1	86.8 ± 0.1
Dense bioglass [15]	–	–	~500	0.5–1	35

4 Conclusions

Porous Al_2O_3/(25 vol.%) m-ZrO_2 bodies were successfully fabricated using 80 vol.% of PMMA as a pore-forming agent. The pores of porous bodies about 200 μm in diameter were homogeneously dispersed in the Al_2O_3/m-ZrO_2 matrix and showed good interconnection between them. Al_2O_3–(m-ZrO_2)/bioglass composites were fabricated by the melt infiltration process using porous Al_2O_3/m-ZrO_2 bodies and molten bioglass. Most Al_2O_3/m-ZrO_2 pores were fully infiltrated by the bioglass. The values of fracture toughness and elastic modulus of the Al_2O_3–(m-ZrO_2)/bioglass composites were 2.35 MPa $m^{1/2}$ and 86.8 GPa, respectively. This is a significant improvement compared to previous results reported in the literature.

Acknowledgement This work was supported by the Korea Science and Engineering Foundation (KOSEF) grant funded by the Korea government (MOST) (No. R01-2007-000-21038-0).

References

1. H. Fischer, C. Niedhart, N. Kaltenborn, A. Prange, R. Marx, F.U. Niethard et al., Biomaterials **26**, 6151 (2005)
2. G. Piconi, C. Maccauro, Biomaterials **20**, 1 (1999). doi:10.1016/S0142-9612(98)00010-6
3. Y.M. Kong, C.J. Bae, S.H. Lee, H.W. Kim, H.E. Kim, Biomaterials **26**, 509 (2005). doi:10.1016/j.biomaterials.2004.02.061
4. S.H. Rhee, Y. Suetsugu, J. Tanaka, Biomaterials **22**, 2843 (2001). doi:10.1016/S0142-9612(01)00028-X
5. W. Xia, J. Chang, J. Non-Cryst. Solids **354**(12), 1338 (2008)
6. F.H. Lin, Y.Y. Huang, M.H. Hon, S.C. Wu, J. Biomed. Eng. **13**(4), 328 (1991)
7. H.A. ElBatal, M.A. Azooz, E.M.A. Khalil, A.S. Monem, Y.M. Hamdy, Mater. Chem. Phys. **80**, 599. doi:10.1016/S0254-0584(03)00082-8
8. Q.Z. Chen, I.D. Thompson, A.R. Boccaccini, Biomaterials **27**, 2414 (2006). doi:10.1016/j.biomaterials.2005.11.025
9. M. Bosetti, M. Cannas, Biomaterials **26**, 3873 (2005). doi:10.1016/j.biomaterials.2004.09.059
10. I.A. Silver, J. Deas, M. Erecinska, Biomaterials **22**, 175 (2001). doi:10.1016/S0142-9612(00)00173-3
11. W. Xia, J. Chang, J. Non-Cryst. Solids **354**, 1338 (2008). doi:10.1016/j.jnoncrysol.2006.10.084
12. G. Goller, H. Demirkiran, F.N. Oktar, E. Demirkesen, Ceram. Int. **29**, 721 (2003). doi:10.1016/S0272-8842(02)00223-7
13. M. Amaral, M.A. Lopes, R.F. Silva, J.D. Santos, Biomaterials **23**, 857 (2002). doi:10.1016/S0142-9612(01)00194-6
14. H.R.R. Ramay, M. Zhang, Biomaterials **25**, 5171 (2004). doi:10.1016/j.biomaterials.2003.12.023
15. H.B. Guo, X. Miao, Y. Chen, P. Cheang, K.A. Khor, Mater. Lett. **58**, 304 (2004). doi:10.1016/S0167-577X(03)00474-9
16. G.D. With, A.J. Corhijn, J. Mater. Sci. **24**, 3411 (1998). doi:10.1007/BF01139073
17. B.T. Lee, S.K. Sarkar, H.Y. Song, J. Eur. Ceram. Soc. **28**, 229 (2008). doi:10.1016/j.jeurceramsoc.2007.05.010
18. B.T. Lee, C.W. Lee, M.H. Youn, H.Y. Song, Mater. Sci. Eng. A **458**, 11 (2007). doi:10.1016/j.msea.2006.11.155
19. B.T. Lee, D.V. Quang, H.Y. Song, J. Korean Ceram. Soc. **44**, 291 (2007)
20. J.K. Han, F. Saito, B.T. Lee, Mater. Lett. **58**, 2181 (2004). doi:10.1016/j.matlet.2004.01.023
21. K. Rezwan, Q.Z. Chen, J.J. Blaker, A.R. Boccaccini, Biomaterials **27**, 3413 (2006). doi:10.1016/j.biomaterials.2006.01.039